Axisymmetric, Primitive Equation, Spectral Tropical Cyclone Model. Part II: Normal Mode Initialization

MARK DEMARIA

National Center for Atmospheric Research, Boulder, CO 80307*

WAYNE H. SCHUBERT

Department of Atmospheric Science, Colorado State University, Fort Collins, CO 80523

(Manuscript received 18 May 1984, in final form 18 January 1985)

ABSTRACT

A three-layer, primitive equation tropical cyclone model is used to test the effect of nonlinear normal mode initialization (NNMI) in a tropical cyclone simulation. The model is solved using a spectral method with normal mode basis functions. Results from a six-day tropical cyclone simulation are used as initial data to test the NNMI. It is shown that Machenhauer's NNMI scheme converges rapidly under tropical cyclone conditions when the dissipative and convective terms are not included in the nonlinear forcing (adiabatic initialization). When these terms are included (diabatic initialization), Machenhauer's scheme no longer converges, but can still reduce the initial gravity mode time tendencies to an acceptable level. The radial winds produced by the diabatic initialization are qualitatively similar to those in the control simulation, but the positioning of the convective heating with respect to the radius of maximum wind is somewhat different. Because of this, the errors in the storm intensity using the control simulation as a perfect forecast are about the same for the adiabatic and diabatic initializations. This indicates that the usefulness of the standard Machenhauer initialization in tropical cyclone models may be limited. The diabatic initialization scheme used in the ECMWF operational model is also tested. For this case, the time-averaged diabatic forcing is determined from a short model run and then held fixed during the iteration. For this case, the diabatic initialization converges and produces a radial wind field consistent with the control simulation.

1. Introduction

Much progress has been made in the initialization of primitive equation models since the introduction of nonlinear mode initialization (NNMI) techniques by Machenhauer (1977) and Baer and Tribbia (1977). These techniques are based on the fact that the normal modes of the linearized primitive equations in spherical geometry can be classified as gravity–inertia or Rossby waves. The basic idea of NNMI is to project the initial data onto the normal modes of the linearized equations. The amplitudes of the gravity–inertia waves are then adjusted so that their initial time tendencies (rather than the amplitudes themselves) are zero. This eliminates spurious gravity wave oscillations which might result from unbalanced initial pressure and wind data.

Machenhauer (1977) and Baer and Tribbia (1977) demonstrated the effectiveness of NNMI in shallow water equation models. These results were generalized to baroclinic models by Andersen (1977) and Daley (1979). An attractive feature of NNMI is that, in principle, it is possible to include physical processes such as dissipation and convective heating in the initialization procedure. For example, Williamson and Temperton (1981) have shown that when surface friction was included in a multilevel grid point model, NNMI produced cross-isobar flow in the lower levels.

Although NNMI has many advantages, it also has some difficulties. Williamson and Temperton (1981) have shown that the iterative procedure introduced by Machenhauer (1977) does not converge when convective heating is included in the nonlinear forcing. Tribbia (1981) has shown that geopotential height constrained initialization (where the gravity wave amplitudes are determined in such a way that the geopotential height field is not changed) fails in regions where the ellipticity condition for the standard nonlinear balance equation is violated. In addition, Ballish (1981) and Errico (1983) have shown that Machenhauer's procedure will diverge in regions where the advective wind speed exceeds the phase speed of the gravity waves. This may present a problem for the initialization of higher internal gravity modes with relatively small phase speeds.

Despite the above difficulties, NNMI schemes have been applied in a number of global prediction models (e.g., Daley, 1979; Puri and Bourke, 1982). Kitade (1983) has suggested a modification to Machenhauer's

* The National Center for Atmospheric Research is sponsored by the National Science Foundation.

iterative procedure which appears to improve the convergence properties of the scheme. Kitade presents several examples of the initialization of a global spectral model which includes dissipative processes and convective heating. These results show that the initialized fields contain reasonable divergent winds when the convective heating is included in the nonlinear forcing.

Although NNMI techniques were originally developed for global prediction problems, they have recently been applied to limited area models by Briere (1982) and Bourke and McGregor (1983). Results from these studies show that many of the results of NNMI for global models also apply for limited area models. This suggests that NNMI techniques may also be useful in tropical cyclone models. As summarized by Elsberry (1979), nearly all operational tropical cyclone models are initialized using the nonlinear balance equation. In some cases, the storm-scale circulation is modified by adding specified tangential and radial wind components. Using these techniques, it is extremely difficult to obtain a consistent divergent wind component. The use of NNMI with physical processes included in the nonlinear forcing may then remove this difficulty.

Hoke and Anthes (1977) have shown that dynamic initialization can be used in operational tropical cyclone models, although it is computationally expensive. Williamson and Temperton (1981) have shown that in a global model, NNMI requires much less computational effort than dynamic initialization, once the model normal modes are determined. The purpose of this paper is to investigate the effect of NNMI in a tropical cyclone model. Because the aim of this work is to study NNMI rather than to simulate all the details of tropical cyclone formation, a physical model with maximum simplification was chosen. The model used here is based on that of Ooyama (1969a,b), and has the simplest geometry (f-plane, axisymmetric) and the minimum vertical resolution (three layers) needed to simulate a tropical cyclone. In addition, Ooyama's model has a relatively simple cumulus parameterization scheme that can still reproduce many aspects of tropical cyclones. A detailed description of the model is given in Schubert and DeMaria (1985, henceforth referred to as Part I).

In Section 2, the governing equations and spectral solution of the model are briefly summarized. The cumulus parameterization and the application of NNMI are also discussed in this section. In Section 3, a tropical cyclone simulation is presented which will be used as a control run to test the NNMI. In Sections 4 and 5, Machenhauer's initialization scheme is applied to the control simulation with and without cumulus parameterization terms included in the nonlinear forcing, and the initialized fields are compared with the control simulation. The impact of the initialization is assessed in Section 6 by comparing model runs with the initialized fields to the control simulation.

2. Governing equations

As described in Part I, the large-scale atmosphere is treated as three axisymmetric incompressible homogeneous fluid layers. The layers have densities $\rho_j = \epsilon_j \rho$ ($j = 0, 1, 2$ and $\epsilon_0 = 1$) with $\rho_0 > \rho_1 > \rho_2$ and thicknesses $H_j + h_j(r, t)$, where the constants H_j are the undisturbed thicknesses at large radii.

The fluid system used here is slightly more general than that of Ooyama (1969a), who assumed the lowest layer had a constant thickness ($h_0(r, t) = 0$) and that $\rho_0 = \rho_1$. These assumptions are relaxed in this study because they have a large effect on the normal modes of the model. DeMaria and Schubert (1984) have derived the normal modes for the incompressible fluid system described here with the assumptions that $h_0 = 0$ and $\rho_0 = \rho_1$ in a model with Cartesian geometry on a mid-latitude β-plane. The normal modes are determined by first finding the vertical normal modes of the linearized equations. Then for each vertical mode, there is a set of equations for the horizontal structure. For the three-layer incompressible fluid system there are three vertical modes. For two of the vertical modes, the horizontal structure equations are analogous to shallow water equations, so that the normal modes can be classified as gravity–inertia or Rossby waves. However, when $h_0 = 0$ and $\rho_0 = \rho_1$, the horizontal structure equations for the third vertical mode simply describe inertial oscillations. This does not present a problem for the integration of the model, but does affect NNMI. This is because the velocity field in the boundary layer is largely represented by this third vertical mode. As described in DeMaria and Schubert, this vertical mode cannot be initialized using Machenhauer's procedure, since the frequencies of the inertial oscillations are relatively slow compared to the gravity wave frequencies of the other vertical modes. Because of this, the initialization scheme cannot produce boundary layer convergence for this case. Since the convective heating is parameterized in terms of the boundary layer convergence, as will be discussed later, the application of NNMI does not interact with the parameterization scheme. Thus, to investigate the effect of NNMI for the case when the cumulus parameterization is involved, the assumptions that $h_0 = 0$ and $\rho_0 = \rho_1$ must be relaxed.

The governing equations for the incompressible fluid system can be written as

$$\frac{\partial u_j}{\partial t} - fv_j + \frac{\partial \phi_j}{\partial r} = f_j \tag{2.1}$$

$$\frac{\partial v_j}{\partial t} + fu_j = g_j \tag{2.2}$$

$$\frac{\partial h_j}{\partial t} + H_j \frac{\partial (ru_j)}{r\partial r} = q_j \tag{2.3}$$

$$\phi_0 = g(h_0 + \epsilon_1 h_1 + \epsilon_2 h_2) \tag{2.4}$$

$$\phi_1 = g\left(h_0 + h_1 + \frac{\epsilon_2}{\epsilon_1} h_2\right) \tag{2.5}$$

$$\phi_2 = g(h_0 + h_1 + h_2) \tag{2.6}$$

where u_j is the radial wind of layer j, v_j the tangential wind of layer j, and f_j, g_j, and q_j contain all the nonlinear and forcing terms as defined in Part I.

The terms f_j, g_j and q_j also contain second- and fourth-order linear diffusion terms, which were not described in Part I. The second-order diffusion terms were included for consistency with Ooyama's original model, and the diffusion coefficient is 10^3 m^2 s^{-1}. The fourth-order diffusion terms (with a diffusion coefficient of 5×10^{12} m^4 s^{-1}) were added for computational reasons. When (2.1)–(2.3) are solved using a spectral method, there is a tendency for the energy of the highest wavenumber modes to become too large. As discussed by Machenhauer (1979), this "spectral blocking" phenomenon can be controlled by the scale-selective diffusion used here. The "spectral blocking" could also have been controlled by making the second-order diffusion coefficient larger. However, the use of a second-order diffusion coefficient large enough to control the blocking resulted in too large a damping of the lower wavenumber modes. Thus, a more scale-selective diffusion was needed.

Diabatic effects are included in the incompressible fluid system by allowing mass to move between layers of different density. In this study, fluid can be transported from layer 1 to layer 2 ($Q^+_{3/2}$), from layer 0 to layer 1 ($Q^+_{1/2}$) and from layer 1 to layer 0 ($Q^-_{1/2}$). Following Ooyama (1969a), the diabatic term $Q^+_{3/2}$ which represents the effects of cumulus convection is given by

$$Q^+_{3/2} = \begin{cases} \eta w & \text{if} \quad w > 0 \\ 0 & \text{if} \quad w \leq 0, \end{cases} \tag{2.7}$$

where w is the vertically-integrated boundary layer convergence given by

$$w = -(H_0 + h_0) \frac{1}{r} \frac{\partial (ru_0)}{\partial r}. \tag{2.8}$$

The proportionality factor η in (2.7) is given by

$$\eta = 1 + \frac{\chi_0 - \chi_2}{\chi_2 - \chi_1} \tag{2.9}$$

where χ_j is the equivalent potential temperature deviation of layer j. In Ooyama's original formulation, χ_0 is obtained from a prognostic conservation equation, χ_1 is set to a constant and χ_2 is diagnosed from the thickness of the upper fluid layer. For simplicity, both χ_0 and χ_1 will be set to constant values of 20 K and −10 K, respectively, which correspond to equivalent potential temperatures of 360 K and 330 K. Following Ooyama, χ_2 is given by

$$\chi_2 = \frac{g\gamma}{c_p} \left(1 - \frac{\epsilon_2}{\epsilon_1}\right) h_2 \tag{2.10}$$

where c_p is the specific heat at constant pressure and the nondimensional parameter γ has a value of about 10.0. Equation (2.10) is derived using an analogy with a compressible fluid and simulates the effect of upper-level warming on the convection.

As discussed previously, Ooyama assumed that layer 0 had a constant thickness and $\rho_0 = \rho_1$. This implies that the mass divergence in layer 0 is compensated by a vertical mass flux between layers 0 and 1. When these assumptions are relaxed, mass divergence in layer 0 results in a change in the thickness of this layer. In regions of boundary layer convergence, the thickness of this layer became unrealistically large, while in regions of boundary layer divergence, the thickness of the layer decreased to zero, and resulted in a numerical instability. To avoid this difficulty, the mass divergence in the boundary layer was compensated by a mass flux between layers 0 and 1. Thus,

$$Q^+_{1/2} = \begin{cases} w & \text{if} \quad w > 0 \\ 0 & \text{if} \quad w \leq 0 \end{cases} \tag{2.11}$$

$$Q^-_{1/2} = \begin{cases} 0 & \text{if} \quad w \geq 0 \\ w & \text{if} \quad w < 0. \end{cases} \tag{2.12}$$

The parameters H_j and ϵ_j were determined as described in Part I. In this study, $H_0 = 737$ m, $H_1 = 4206$ m, $H_2 = 3835$ m, $\epsilon_1 = 0.8758$ and $\epsilon_2 = 0.7683$. With these values of H_j and ϵ_j, the pure gravity wave speeds for the three vertical modes are 287, 52 and 28 m s^{-1}, and the fractions of the basic state total column mass in layers 0, 1, and 2 are $1/10$, $5/10$ and $4/10$, respectively.

The governing equations (2.1)–(2.3) were solved using a spectral method where the normal modes of the linearized equations ($f_j = g_j = q_j = 0$) were used as basis functions, as described in Part I.

The first step is to transform (2.1)–(2.3) in the vertical so that the dependent variables are amplitudes of vertical normal modes. When this is done, the governing equations for each vertical mode are of the form of shallow water equations with pure gravity wave speed c_m, where $m = 0$, 1 or 2 is the vertical mode number. As discussed previously, c_m takes the value of 287, 52 or 28 m s^{-1} for $m = 0$, 1, or 2.

The next step is to expand the vertically transformed dependent variables in a series of the eigenfunctions of the horizontal linear operator which appears in the vertically transformed governing equations. As described in Part I, these eigenfunctions can be written as three-component vectors, where each component

is either a zero- or first-order Bessel function of the first kind.

Once the horizontal transform is applied, the governing equations become

$$\frac{dW_{mns}}{dt} + i\nu_{mns}W_{mns} = N_{mns} \tag{2.13}$$

where W_{mns} is a normal mode amplitude, ν_{mns} a normal mode frequency and N_{mns} the amplitude of the normal mode projection of the nonlinear and forcing terms. The normal mode frequencies are given by

$$\nu_{mns} = \begin{cases} 0, & s = 0 \quad \text{(geostrophic modes)} \\ -(f^2 + c_m^2 k_{mn}^2)^{1/2}, & s = 1 \\ (f^2 + c_m^2 k_{mn}^2)^{1/2}, & s = 2 \\ & \text{(gravity-inertia modes)} \end{cases} \tag{2.14}$$

where k_{mn} ($n = 1, 2, \cdots$) are discrete wavenumbers determined by application of the lateral boundary condition at $r = a$. Equation (2.13) is the normal mode form of the original governing equations where W_{mns} represents the amplitudes of the geostrophic modes ($s = 0$) or gravity modes ($s = 1, 2$).

Equation (2.13) was solved using second-order Adams-Bashforth time differencing with an initial forward time step. In all of the simulations in the following sections, the horizontal series was truncated at $N = 64$ with $a = 800$ km. The nonlinear terms N_{mns} were calculated using the transform method (Orszag, 1970; Eliasen *et al.*, 1970) using $3N + 1$ evenly spaced grid points. With $a = 800$ km, the spacing of the transform grid is then about 4 km.

When the governing equations are written in normal mode form as in (2.13) the application of the NNMI scheme proposed by Machenhauer (1977) is straightforward. The first step is to divide W_{mns} into a slow mode (low frequency) part and a fast mode (high frequency) part. With the simple f-plane geometry used here, the geostrophic modes ($s = 0$) can be considered the slow modes and the gravity modes ($s = 1, 2$) the fast modes. Then for Machenhauer's initialization scheme, the amplitudes of the slow modes are not changed, while the amplitudes of the fast modes are determined by assuming that dW_{mns}/dt is small enough so that (2.13) becomes

$$W_{mns} = -\frac{i}{\nu_{mns}} N_{mns}, \quad s = 1, 2. \tag{2.15}$$

Since N_{mns} in (2.15) is a nonlinear function of W_{mns}, this equation is solved using an iterative procedure described by

$$W_{mns}^{(r+1)} = -\frac{i}{\nu_{mns}} N_{mns}^{(r)}, \quad s = 1, 2, \tag{2.16}$$

where the superscript r is the iteration number. In all of the results to be presented, W_{mns} for $s = 1, 2$ was set to zero before the iteration scheme (2.16) was applied.

As discussed in Section 1, there are many cases where (2.16) does not converge. Kitade (1983) has suggested a modification to (2.16) given by

$$W_{mns}^{(r+1)} = (1 - \omega)W_{mns}^{(r)} - \frac{i\omega}{\nu_{mns}} N_{mns}^{(r)} \tag{2.17}$$

where ω can be interpreted as an under-relaxation parameter. In all of the subsequent discussion, (2.17) will be referred to as the K-scheme while (2.16) will be referred to as the M-scheme. When $\omega = 1$ in (2.17), the K-scheme is equivalent to the M-scheme. Kitade used a value of $\omega = 0.5$.

In addition to the inclusion of an under-relaxation parameter in the iterative scheme, Kitade used a 48-hour period cutoff. That is, only the modes with periods shorter than 48 hours were initialized. In the axisymmetric model, only the gravity modes are initialized. Since the "slowest" gravity mode in the model has a period of about 16 hours, the initialization scheme used here is consistent with Kitade's.

3. Control simulation

In this section, a tropical cyclone simulation using the spectral model described previously is presented. The results from this simulation will be used as a control to test the effect of the NNMI. The initial mass and wind fields for this simulation are given by

$$u_j = 0, \quad j = 0, 1, 2 \tag{3.1}$$

$$v_j = \begin{cases} 2v_m\left(\frac{r}{r_m}\right)\left[1 + \left(\frac{r}{r_m}\right)^2\right]^{-1}, & j = 0, 1 \\ 0, & j = 2 \end{cases} \tag{3.2}$$

$$\phi_j = \begin{cases} -2v_m^2[1 + (r/r_m)^2]^{-1} + fv_m r_m \\ \qquad \times \ln[1 + (r/r_m)^2], & j = 0, 1 \\ 0, & j = 2 \end{cases} \tag{3.3}$$

where the maximum tangential wind $v_m = 6.0$ m s^{-1} at a radius $r_m = 60$ km. The initial condition defined by (3.1)–(3.3) is a weak axisymmetric vortex in gradient wind balance with no initial radial circulation.

In the incompressible fluid system, the deviation from the mean surface pressure is given by

$$P_s = \rho g(h_0 + \epsilon_1 h_1 + \epsilon_2 h_2) = \rho\phi_0. \tag{3.4}$$

Figure 1 shows the time evolution of P_s (assuming $\rho = 1.0$ kg m^{-3}) and the maximum layer 1 tangential wind for the control simulation. This figure shows that the initial vortex slowly develops during the first 48 hours of the simulation. Between 48 and 96 hours, the vortex intensifies more rapidly and reaches hurricane strength ($v_1 \geq 33$ m s^{-1}) by about 60 hours. After 96 hours, the intensity of the vortex slowly decreases.

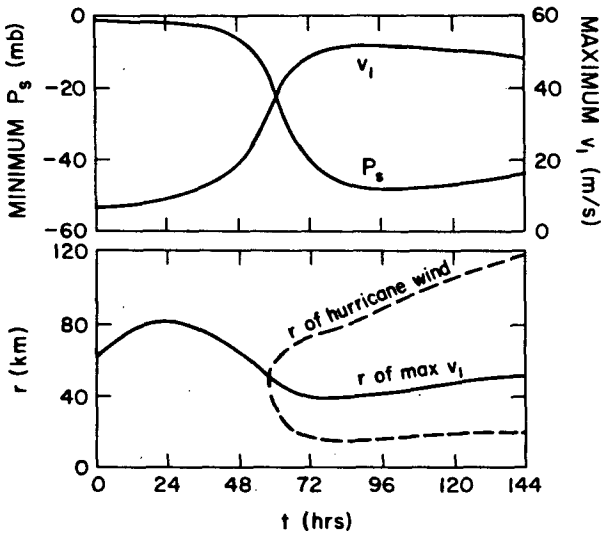

FIG. 1. The time evolution of the minimum surface pressure deviation (P_s) and maximum layer 1 wind speed and the time evolution of the radius of maximum wind and radii of hurricane wind for the control simulation.

The lower portion of Fig. 1 shows the radius of maximum tangential wind and the radii of hurricane force wind (v_1 = 33 m s^{-1}). During the first 24 hours, the radius of maximum wind expands to about 80 km. During the next 48 hours, it contracts to less than 40 km and then slowly expands after this time. By 96 hours, the model has produced a mature tropical cyclone with a minimum surface pressure of about 960 mb (asuming a mean surface pressure of 1010 mb) with a maximum tangential wind of 52 m s^{-1} at a radius of 40 km. These values are consistent with observations from the inner regions of tropical cyclones presented by Shea and Gray (1973).

Figure 2 shows the radial structure of u_j, v_j, and ϕ_j at 48 and 96 hours. This figure shows that the radial circulation is characterized by strong boundary layer inflow, weaker inflow in layer 1 and outflow in layer 2. The tangential circulation is cyclonic in all the layers in the inner regions of the storm ($r \leqslant 200$ km) with an anticyclone in layer 2 in the outer regions.

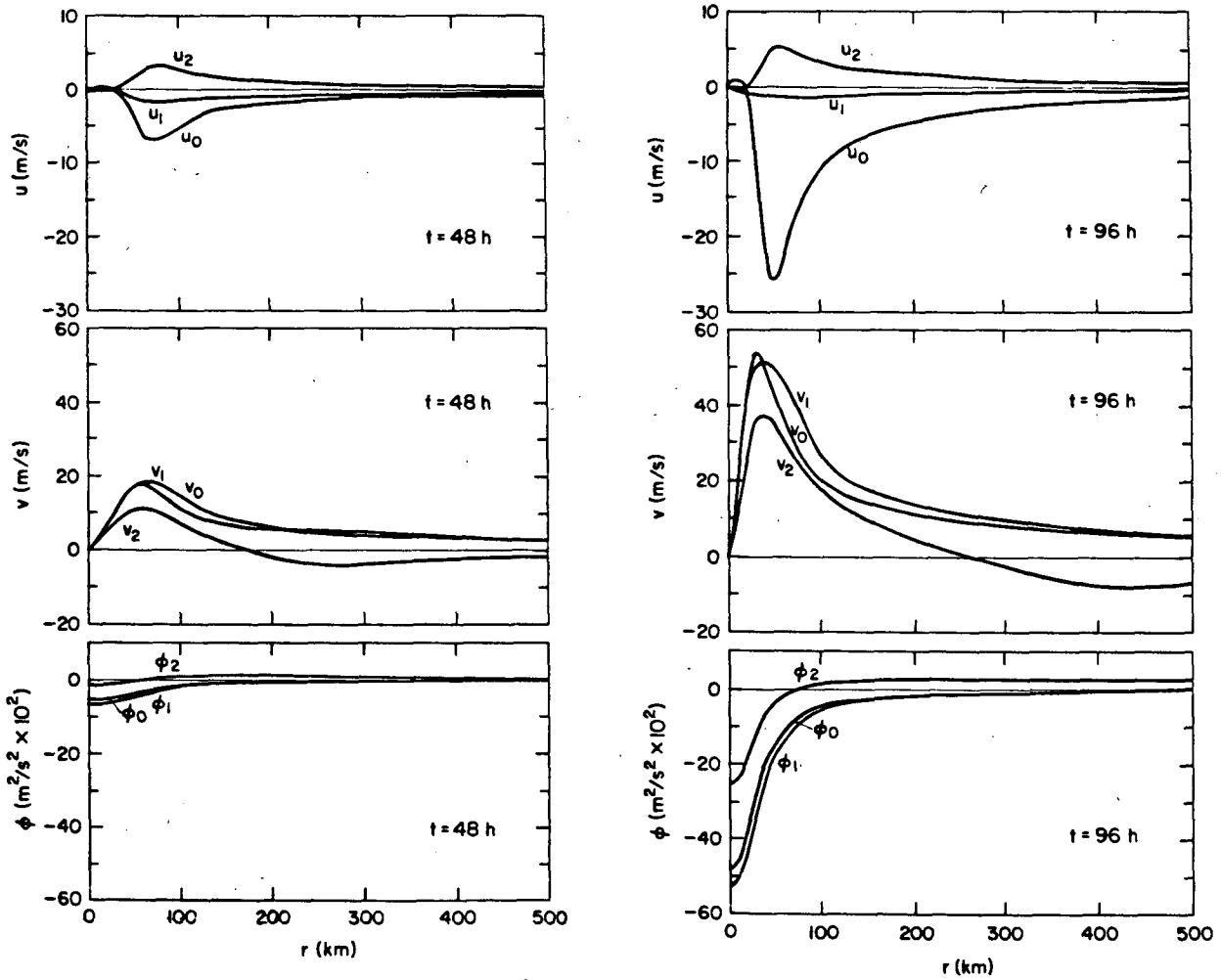

FIG. 2. The radial and tangential winds and geopotential (u, v and ϕ) for layers 0, 1 and 2 as a function of radius for the control simulation at t = 48 hours and t = 96 hours.

Figure 3 shows the nondimensional absolute vorticity Z_j defined by

$$Z_j = \left[\frac{\partial(rv_j)}{r\partial r} + f\right] f^{-1} \tag{3.5}$$

for layers 1 and 2 at 48 and 96 hours. This figure shows that by 48 hours, a region of negative absolute vorticity ($Z_j < 0$) has formed in layer 2. By 96 hours, the region of negative absolute vorticity in layer 2 has increased in size and a small region also exists in layer 1.

As discussed in Section 1, Tribbia (1981) has shown that geopotential height constrained NNMI will fail in regions where the ellipticity condition for the nonlinear balance equation is violated. In the axisymmetric model, non-elliptic regions can be interpreted in terms of the gradient wind equation. When $\partial\phi/\partial r$ is less than a critical value $(\partial\phi/\partial r)_c$, it is no longer possible to find a tangential wind which satisfies the gradient wind equation. It is straightforward to show that $(\partial\phi/\partial r)_c$ is given by

$$\left(\frac{\partial\phi}{\partial r}\right)_c = -\frac{f^2 r}{4} \tag{3.6}$$

so that the criterion for obtaining gradient balanced winds is given by

$$\frac{\partial\phi}{\partial r} \geqslant -\frac{f^2 r}{4}. \tag{3.7}$$

Taking $(fr)^{-1}\partial(r)/\partial r$ of (3.7) gives

$$\frac{1}{f}\frac{\partial}{r\partial r}\left(r\frac{\partial\phi}{\partial r}\right) = \frac{1}{f}\nabla^2\phi \geqslant -\frac{f}{2} \tag{3.8}$$

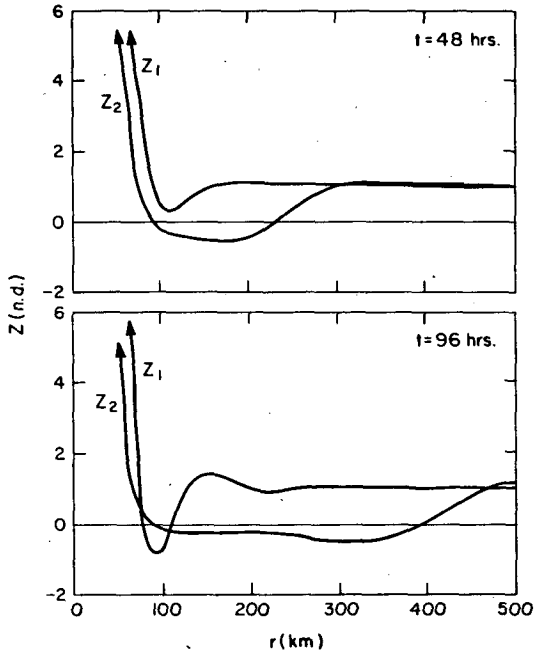

FIG. 3. The nondimensional absolute vorticity (Z) for layers 1 and 2 as a function of radius for the control simulation at t = 48 hours and t = 96 hours.

which is the standard ellipticity condition for the nonlinear balance equation.

Figure 4 shows $\partial\phi/\partial r$ and $(\partial\phi/\partial r)_c$ as a function of radius for layer 2 at 48 and 96 hours. This figure shows that at these times, $\partial\phi/\partial r$ always exceeds $(\partial\phi/\partial r)_c$ so that it would be possible to obtain balanced winds from the geopotential. This condition is also satisfied in layers 0 and 1, since $\partial\phi/\partial r$ is always positive as can be seen in Fig. 2.

As described in Section 2, the NNMI procedure assumes that the dW_{mns}/dt term in (2.13) is small compared to the other two terms. The convergence of the iterative scheme used in the NNMI can be evaluated by calculating the parameter B_G given by

$$B_G = \sum_{m=0}^{2}\sum_{n=1}^{N}\sum_{s=1}^{2}\left|\frac{dW_{mns}}{dt}\right|^2. \tag{3.9}$$

Note that the summation in the above equation is for the gravity modes only since s = 1, 2. For comparison with B_G, the sum of the square of the second term in (2.13) can also be calculated for the gravity modes using

$$A_G = \sum_{m=0}^{2}\sum_{n=1}^{N}\sum_{s=1}^{2}\nu_{mns}^2|W_{mns}|^2. \tag{3.10}$$

Figure 5 shows the time evolution of B_G and A_G for the control simulation. This figure shows that during most of the simulation, A_G is more than two orders of magnitude larger than B_G. This suggests that during the model simulation the first term in (2.13) remains fairly small compared to the second term. This indicates that the gravity mode amplitudes obtained by the NNMI should be a good approximation to those obtained from the control simulation.

Leith (1980) introduced the slow manifold which is defined as the set of model states which are evolving slowly in time. NNMI can then be interpreted as adjusting the initial model state so that it is as close as possible to the slow manifold. In the initialization experiments in the following sections, it is assumed that the model state during the control simulation is close to the slow manifold. The model state is then moved off the slow manifold by setting the gravity mode amplitudes to zero. It is then possible to determine if the M-scheme (2.16) or the K-scheme (2.17) is capable of moving the model state back towards the slow manifold by comparing the initialized model results to the uninitialized control simulation.

The results from the control simulation suggest that with an initial condition of a weak vortex in gradient balance, the model state remains close to the slow manifold. In the axisymmetric model, the radial wind projects entirely onto the gravity modes, while the tangential wind projects almost entirely onto the geostrophic modes. This was verified by constructing u_j and v_j from the spectral amplitudes W_{mns} with either the gravity or geostrophic modes set to zero. Thus, the time evolutions of the radial and

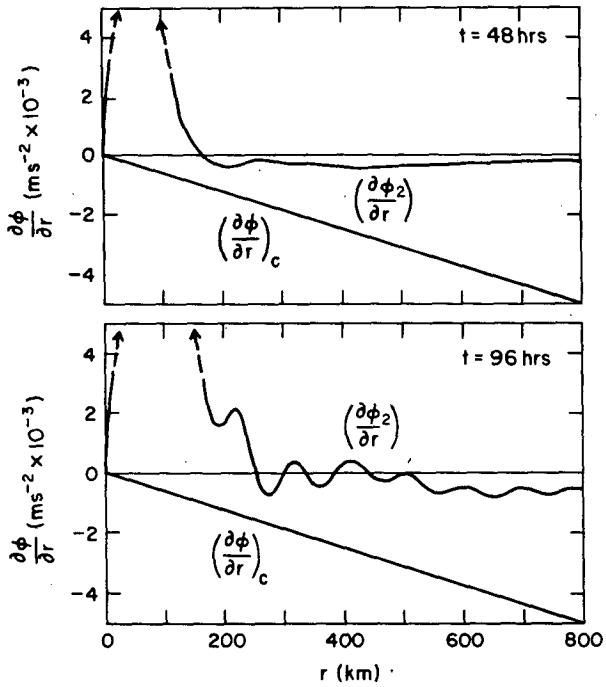

FIG. 4. The radial gradient of the layer 2 geopotential ($\partial\phi_2/\partial r$) as a function of radius for the control simulation at t = 48 hours and t = 96 hours. Also shown is the minimum value of the geopotential gradient for which gradient balanced tangential winds exist $(\partial\phi/\partial r)_c$.

tangential winds provide estimates of the time evolutions of the gravity and geostrophic modes. In the control simulation the time evolutions of the radial and tangential winds are quite similar in that it required about 96 hours for the intense radial and tangential circulations shown in Fig. 2b to develop. The radial wind does not show any significant amplitude higher frequency oscillations, which indicates that the time scale of the gravity modes is the same as the time scale of the geostrophic modes, rather than the time scale of the gravity mode frequencies (ν_{mns}, s = 1, 2) which have corresponding periods ranging from about 16 hours to 90 seconds. Assuming that the slow manifold is defined by the time scale of the geostrophic modes, the above results suggest that the model state in the control simulation does remain close to the slow manifold.

4. Adiabatic initialization

Tribbia (1981) has shown in a highly truncated axisymmetric spectral model that adiabatic geopotential constrained NNMI is equivalent to obtaining the tangential wind from the geopotential using the gradient wind equation. Thus, the application of the M-scheme results in a vortex in gradient wind balance with no radial wind.

This was verified using the current model where the M-scheme was applied to the results from the control simulation at t_i = 0, 48 and 96 hours. For the adiabatic initialization, all the gravity modes were set to zero, and then diagnosed using (2.16), where the N_{mns} term was calculated with the surface drag, horizontal and vertical diffusion, and the diabatic terms $Q^{+}_{3/2}$, $Q^{+}_{1/2}$ and $Q^{-}_{1/2}$ all set to zero. In each case the iteration converged quite rapidly (B_G was reduced by at least ten orders of magnitude after eight iterations), and the resulting solutions contained a zero radial wind and a vortex in gradient wind balance.

In the scheme applied by Tribbia, the geopotential was held constant (constrained initialization). In the unconstrained initialization used here, both the wind and mass fields can vary during the initialization. The unconstrained adiabatic initialization produced very small changes in the tangential wind (rms differences between the initialized and uninitialized tangential winds were less than 0.7 m s^{-1} for t_i = 0, 48 or 96 hours), and adjusted the mass field to obtain gradient balance.

5. Diabatic initialization

Although the M-scheme converged for the adiabatic case, the initialization did not produce a radial wind field. In this section, the M-scheme is applied to the results from the control simulation at t_i = 48 and 96 hours for the case where the friction and mass transport terms are included in the nonlinear forcing. The only terms which are not included in the nonlinear forcing for this case are the fourth-order diffusion terms, since they result in a rapid divergence of the

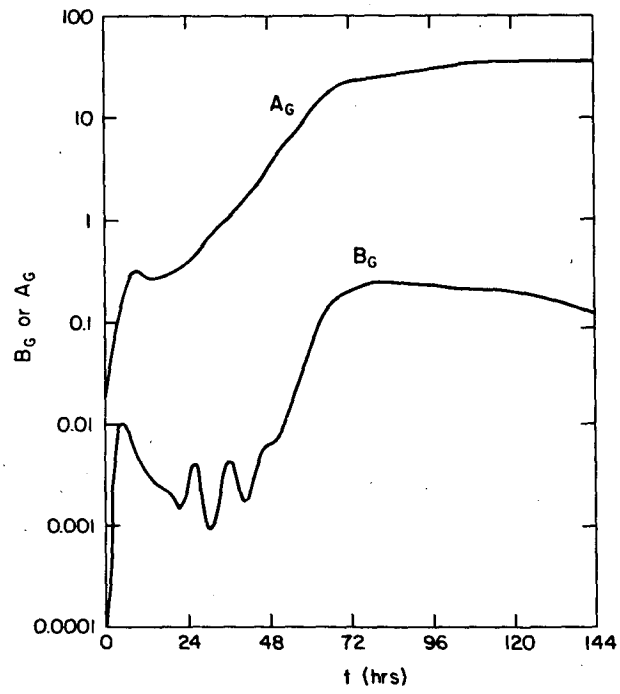

FIG. 5. The time evolution of the summation of the squares of the gravity mode time tendencies (B_G) and the product of the gravity mode amplitudes and frequencies (A_G) for the control simulation.

M-scheme. This divergence occurs because for the fourth-order diffusion there is a term of the form $\lambda k_{mn}^4 W_{mns}$ (where λ is the fourth-order diffusion coefficient) included in the N_{mns} term in (2.16). For some of the high wavenumber modes, the factor $\lambda k_{mn}^4/\nu_{mns}$ is greater than one, so the gravity mode amplitudes are increased by each iteration.

The solid lines in Fig. 6 show the parameter B_G after each iteration of the M-scheme at t_i = 48 and 96 hours. This figure shows that the value of B_G decreases initially, but eventually increases and the iterative solution diverges. This result is somewhat different from the results presented by DeMaria and Schubert (1984) who showed that the M-scheme converged in a three-layer tropical cyclone model with similar moist physics. As discussed in Section 2, however, the boundary layer was assumed to have a constant thickness in this previous study, so that the modes which described most of the inflow in the boundary layer could not be initialized. Because of this, the boundary layer inflow, and thus the convective forcing term $Q_{3/2}^+$, was specified before the initialization procedure was applied. However, the convergence of the iteration obtained in the previous study no longer occurs for the case when the initialization procedure interacts with the cumulus parameterization scheme.

As described in Section 2, Kitade (1983) has suggested a modification to the M-scheme which appears to improve its convergence properties. The K-scheme

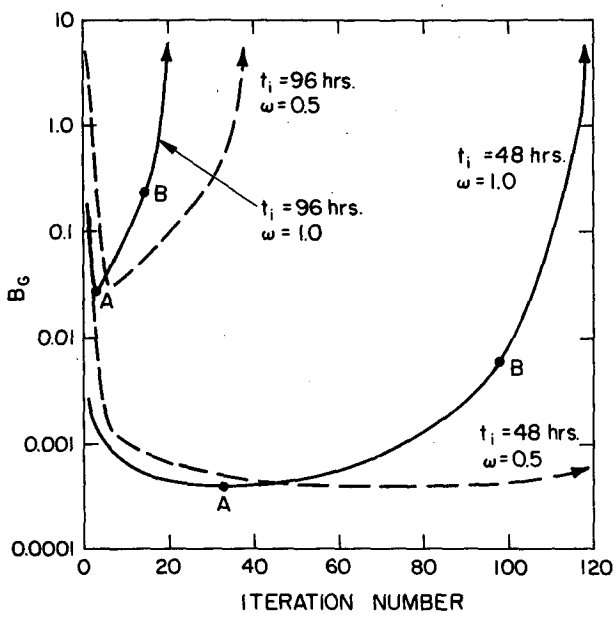

FIG. 6. The summation of the squares of the gravity mode time tendencies (B_G) after each iteration of the M-scheme (solid) and the K-scheme with ω = 0.5 (dashed) for the diabatic initialization of the control simulation at t_i = 48 and 96 hours. The points A and B indicate the value of B_G when the iteration was stopped in the diabatic A and B procedures.

defined by (2.17) was applied to the control simulation with the under-relaxation parameter ω = 0.5. The dashed lines in Fig. 6 show the parameter B_G after each iteration of the K-scheme. This figure shows that the behavior of the K-scheme is quite similar to the M-scheme, except that it diverges after a larger number of iterations. The K-scheme does not reduce B_G to a value lower than the minimum value obtained by the M-scheme, so that it does not appear to be a useful modification in this case.

The K-scheme was also applied with ω = 0.75 and ω = 0.25. The results for these cases were similar to the ω = 0.5 case in that the divergence occurred after a larger number of iterations than for the M-scheme, but the minimum value of B_G was not reduced.

Although the M-scheme eventually diverges, it can be seen in Fig. 6 that the value of B_G during the iteration remains below its value in the control simulation until iteration 98 for t_i = 48 hours and iteration 14 for t_i = 96 hours (indicated by the B points on the solid curves). It may then still be possible to use NNMI if the iteration is stopped when B_G reaches some specified threshold. In this study, two cases will be considered. The most obvious choice is to stop the iteration as soon as B_G begins to increase. As can be seen in Fig. 6, this occurs after 35 iterations for t_i = 48 hours and after three iterations for t_i = 96 hours (indicated by the A points). This procedure will be referred to as diabatic A. The second case which is considered is to stop the iteration when B_G reaches its value in the control simulation after the point where B_G was a minimum. This procedure will be referred to as diabatic B.

Figure 7 shows the radial velocity components after the diabatic A and diabatic B procedures were applied at t_i = 48 hours. Since the gravity modes were set to zero initially, the radial winds are entirely a result of the initialization procedures. Comparing Fig. 7 with Fig. 2 it can be seen that the radial winds are in qualitative agreement with those from the control simulation, in that there is strong inflow in layer 0, weaker inflow in layer 1 and outflow in layer 2. It can also be seen that amplitudes of the radial winds are close to those in the control simulation for the diabatic B case, while they are underestimated for the diabatic A case.

Figure 8 shows the radial wind components after the diabatic A and diabatic B procedures were applied at t_i = 96 hours. Comparing Fig. 8 with Fig. 2 it can be seen that the results for t_i = 96 hours are similar to the results for t_i = 48 hours, except that the underestimation of the amplitudes of the radial winds by the diabatic A procedure is more noticeable. This indicates that in some cases it may be useful to continue the iteration even though the value of B_G is increasing.

The above result shows that the amplitudes of the radial wind fields are closer to those in the control

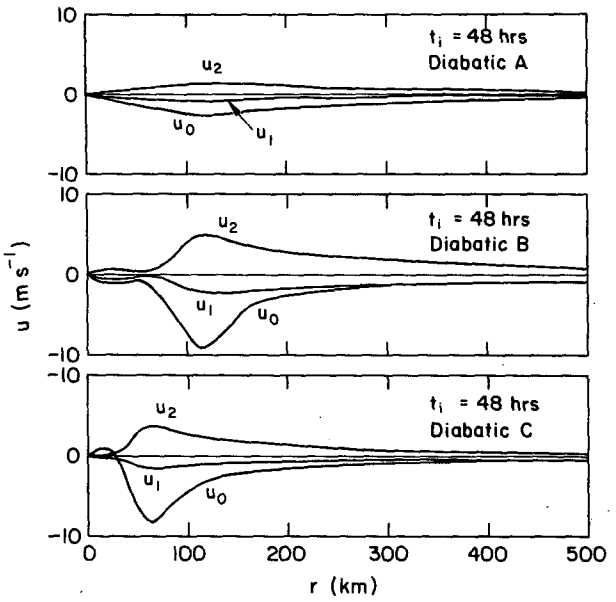

FIG. 7. The radial wind (u) for layers 0, 1 and 2 as a function of radius produced by the diabatic A, diabatic B and diabatic C initializations of the control simulation at t_i = 48 hours.

simulation when the iteration is continued until B_G reaches its value in the control simulation. If this technique were applied in an operational model, the threshold value of B_G would not be known, so that a different criterion would be necessary. One possibility would be to continue the iteration until the integrated diabatic heating produced by the model reaches some specified threshold. In some cases it might be possible to obtain the diabatic heating threshold from observed precipitation rates which can be estimated from satellite observations (e.g., Adler and Rodgers, 1977). In an operational model, however, the computing time would also have to be considered, since at t_i = 48 hours, the diabatic B procedure required 98 iterations.

The diabatic initialization procedures also resulted in changes in the tangential wind and mass fields. Similar to the adiabatic case, the changes in the tangential wind were very small (less than 0.4 m s^{-1}) with the mass field adjusting towards gradient balance.

Although the radial circulations produced by the initialization procedures are qualitatively similar to those in the control simulation, it can be seen that the maximum absolute values of u occur at too large a radius. Since the diabatic heating term $Q_{3/2}^{+}$ is parameterized in terms of the boundary layer convergence, which is a function of u_0, the resulting initial diabatic heating fields are somewhat different from those in the control run. Figure 9 shows the mass transport term $Q_{3/2}^{+}$ for the control simulation and after the diabatic A and diabatic B procedures were applied at t_i = 48 and 96 hours. This figure shows that at both times, the diabatic A procedure underestimates the magnitude of $Q_{3/2}^{+}$ and the maximum value occurs at too large a radius. The diabatic B procedure increases the magnitude of $Q_{3/2}^{+}$, but the maximum value still occurs at too large a radius.

The dashed vertical line RMW in Fig. 9 indicates the radius of maximum layer 1 tangential wind. For the control simulation, much of the diabatic heating occurs inside the RMW while after the initialization is applied, most of the heating occurs outside the RMW. (The effect of the initialization on the RMW is extremely small.) Schubert and Hack (1982) have shown that diabatic heating produces balanced flow more efficiently in inertially stable regions. Since the inertial stability is proportional to the absolute vorticity, it might be expected that the tropical cyclone would intensify more rapidly when the diabatic heating occurred in regions where the absolute vorticity is large. As can be seen in Fig. 3, the absolute vorticity becomes very large inside the radius of maximum wind. It might then be expected that the intensification rate of the tropical cyclone would be reduced by the initialization procedures since the diabatic heating occurs away from the region where the absolute vorticity is large. This will be verified in Section 6 when the model is run using the initialized fields.

The divergence of the M-scheme when physical processes are included in the nonlinear forcing is consistent with the results from global models (e.g., Williamson and Temperton, 1981). A technique used to overcome this difficulty in the ECMWF operational

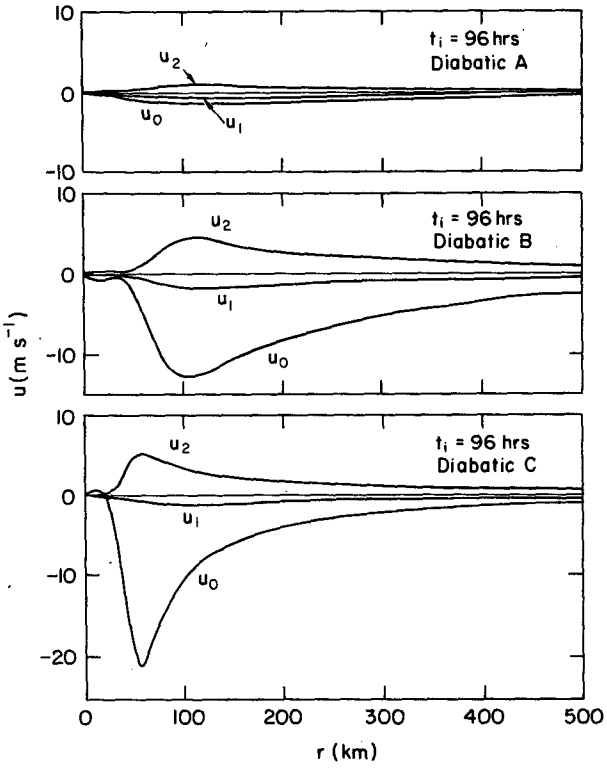

FIG. 8. As in Fig. 7 except for t_i = 96 hours.

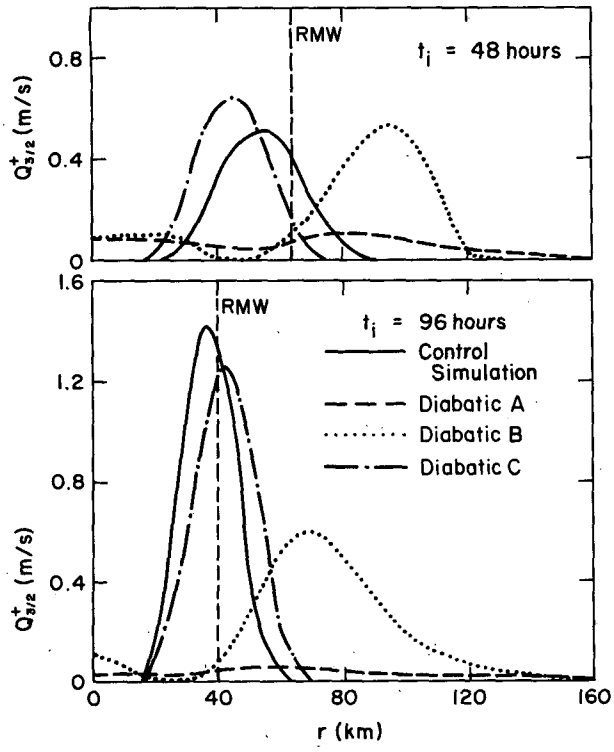

FIG. 9. The mass transport term $Q^+_{3/2}$ as a function of radius for the control simulation and for the diabatic initializations of the control simulation at t_i = 48 hours and t_i = 96 hours. The dashed vertical line RMW indicates the radius of maximum layer 1 tangential wind.

model is to make the diabatic forcing independent of the iteration (Wergen, 1983). For this purpose, the time-averaged diabatic forcing terms are computed during a two-hour forecast started from the uninitialized analysis. If this technique were used in an operational tropical cyclone model, the uninitialized analysis would probably not contain divergent winds near the storm center. Thus, in this study, the uninitialized analysis is taken to be a vortex in gradient wind balance, obtained by applying the adiabatic M-scheme to the control simulation. The model was then run for 12 hours (two hours as used in the ECMWF scheme was found to be inadequate to produce significant amplitude forcing) and the average diabatic forcing was computed. The M-scheme was then applied using this average diabatic forcing in the nonlinear term N_{mns}. This procedure will be referred to as diabatic C.

When the diabatic C procedure was applied at t_i = 48 hours and t_i = 96 hours, the iteration converged about as rapidly as for the adiabatic initialization. The radial winds produced by this scheme are shown in Figs. 7 and 8. Comparing these figures with Fig. 2 shows that the diabatic C procedure provides a more accurate estimate of the radial winds than the diabatic A or B procedures. The dot-dashed line in Fig. 9 shows the mass transport term $Q^+_{3/2}$ after the diabatic C procedure was applied. For t_i = 48 hours and t_i = 96 hours, the maximum value of $Q^+_{3/2}$ is much closer to the RMW, which is more consistent with the control simulation. Thus, at the expense of an extra 12-hour model simulation, the diabatic C scheme produces an initial heating field which is fairly close to that in the control simulation.

6. Impact of initialization on the control simulation

As a simple test of the initialization procedures discussed in the previous sections, the model is run with the initialized fields and the results are compared to the control simulation.

Figure 10 shows the difference in the minimum surface pressure from that in the control simulation (ΔP_s) for 48-hour model runs initialized using the adiabatic, diabatic A, diabatic B and diabatic C procedures. For t_i = 48 hours in Fig. 10 it can be seen that ΔP_s is much smaller for the diabatic C procedure than for the other initialization procedures during the first 30 hours of the model simulations. A similar result can be seen for t_i = 96 hours during the first 18 hours of the simulations.

The reason the simulations initialized using the diabatic A and B procedures resulted in large differences in the surface pressure compared to the control simulation appears to be related to the position of the initial heating in relation to the RMW, as described previously. The differences for the adiabatic initialization are caused by starting the simulation with

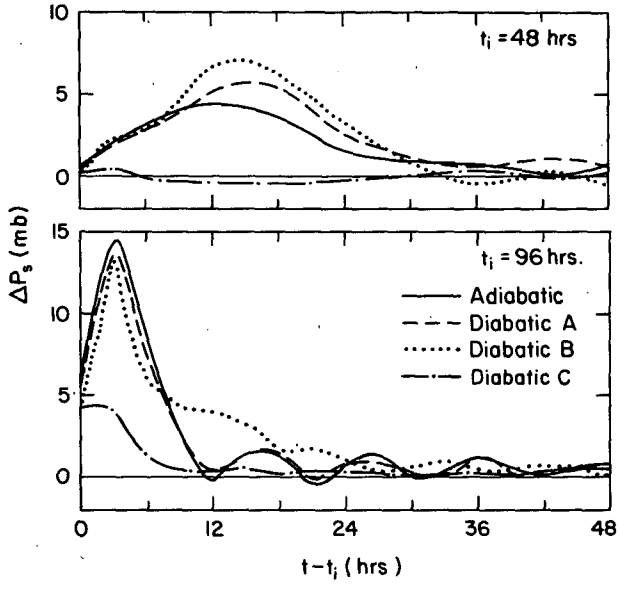

FIG. 10. The time evolution of the difference between the minimum surface pressure in the control simulation and the simulations initialized with the adiabatic and diabatic procedures at t_i = 48 hours and t_i = 96 hours. A positive value of ΔP_s indicates a higher surface pressure in the initialized simulations.

$Q^{+}_{3/2} = 0$. This indicates that the intensity of the model tropical cyclone is extremely sensitive to the initial radial distribution of the diabatic heating. Although the diabatic A and B procedures result in an initial diabatic heating field, the errors introduced by these initializations are about as large as for the adiabatic initialization. Thus, it appears that only the diabatic C procedure is significantly better than applying an adiabatic initialization.

The time evolution of the minimum surface pressure for the control simulation in Fig. 1 shows that P_s does not exhibit any large amplitude oscillatory behavior. In Fig. 10, however, ΔP_s does exhibit oscillatory behavior in the first 24 hours after the adiabatic, diabatic A and diabatic B initialization procedures were applied. This suggests that the model states after these initialization procedures were applied were no longer close to the slow manifold. One possible explanation is that the assumption of zero gravity wave amplitude time tendencies (which gives 2.15) is not a good approximation to the slow manifold in these cases. A second possibility is that (2.15) is a valid approximation of the slow manifold, but that the iterative procedures (2.16) or (2.17) do not provide an accurate solution of this equation. These possibilities will be studied using a highly truncated version of the model.

7. Concluding remarks

The three-layer axisymmetric tropical cyclone model presented by Ooyama (1969a,b) was used to test the effect of NNMI on a tropical cyclone simulation. For this purpose, Ooyama's balance model was written in terms of primitive equations and the assumption of a constant depth boundary layer was relaxed. For simplicity, the boundary layer equivalent potential temperature treated as a prognostic variable in Ooyama's formulation was set to a constant. The governing equations were solved using the spectral (Galerkin) method with normal mode basis functions, as described in Part I. This made the application of the NNMI procedure introduced by Machenhauer (1977) straightforward.

A simulation of the development of a tropical cyclone with maximum tangential winds of about 50 m s^{-1} was used as a control for the NNMI. The results from this simulation were used as initial data so that the effect of NNMI could be evaluated by comparing the initialized fields to the original fields.

When the diabatic forcing and friction terms were not included in the nonlinear terms (adiabatic initialization) Machenhauer's scheme converged quite rapidly under tropical cyclone conditions. The adiabatic initialization resulted in zero radial winds (and thus no initial vertical motion), changed the tangential winds very slightly and adjusted the mass field to obtain gradient balance.

When the diabatic forcing and friction terms were included in the nonlinear terms (diabatic initialization), Machenhauer's scheme no longer converged. The scheme was, howewver, capable of reducing the time tendencies of the gravity modes below the level of the tendencies in the control simulation. Thus, although the initialization cannot reduce the initial gravity mode time tendencies to zero, it can reduce them to an acceptable level.

Kitade (1983) suggested a modification to Machenhauer's scheme to improve its convergence properties. It was shown that for Kitade's modified scheme, divergence occurred after a larger number of iterations, but the minimum value of the gravity mode time tendencies obtained was about the same as for Machenhauer's scheme. Thus, Kitade's scheme does not appear to be a useful modification for the diabatic initialization of the tropical cyclone model.

When the diabatic initialization was stopped after a specified number of iterations, the initialized fields contained radial winds which were qualitatively similar to those from the control simulation (strong boundary layer inflow, weaker midlevel inflow and upper level outflow). It was also shown that the amplitudes of the initialized radial wind fields were closer to those in the control simulation when the iteration was continued beyond the point where the gravity mode time tendencies were minimized. For this case, the iteration was stopped when the tendencies reached the level of the tendencies in the control simulation.

Although the radial wind field produced by the diabatic initialization was qualitatively similar to that in the control simulation, the resulting diabatic heating field was somewhat different. Most of the diabatic heating produced by the initialization occurred outside the radius of maximum tangential wind while much of the diabatic heating occurred inside the radius of maximum wind for the control simulation. When the model was run with the initialized fields, the storm intensity decreased rapidly during the first 6–12 hours of the simulations for adiabatic and the diabatic initializations. This result indicates that the straightforward application of Machenhauer's initialization scheme would probably be of limited usefulness in tropical cyclone models with parameterized moist physics.

The diabatic initialization scheme used in the ECMWF operational model (diabatic C) was also tested. For this case, an adiabatic initialization was first applied to the control simulation to achieve gradient balance. The model was then run for 12 hours and the time-averaged diabatic forcing was calculated. Using this diabatic forcing, the M-scheme converged rapidly, and produced an initial radial wind field which was more consistent with the control simulation. Using this initialization, the intensity of the vortex remained much closer to that in the

control simulation than for the other initialization procedures.

The above result suggests that NNMI using the time-averaged diabatic heating might be useful for the initialization of operational tropical cyclone models such as the moveable fine mesh (MFM) model, which contains parameterized moist physics (Hovermale and Livezey, 1977). A disadvantage of the diabatic C initialization is that it requires more computational effort, since the model must be run for about 12 hours to obtain the average diabatic forcing. It remains to be seen whether this extra computational effort would produce more accurate track forecasts.

A difficulty which might occur in a three-dimensional model which does not occur in the axisymmetric model is related to the storm motion. If the storm was moving, the time-averaged diabatic forcing would be smoothed over some distance since at any particular time it would be concentrated near the storm center. It might be possible to overcome this difficulty by holding the geostrophic modes fixed during the initial 12-hour integration. When this was done in the axisymmetric model, the radial circulation produced by the initialization was very similar to that produced when the geostrophic modes were allowed to vary. The advantage of this in a three-dimensional model is that the storm should remain approximately stationary during the initial integration.

Ooyama's model was used in this study because of its simplicity. In addition, the normal mode spectral solution made the NNMI fairly simple to apply. In a model such as the MFM, which is solved using finite differencing and has time-dependent lateral boundary conditions, the initialization would be considerably more difficult to apply. It may be possible, however, to overcome these difficulties as shown by Temperton and Williamson (1981) who determined the normal modes of a global grid point model, and by Briere (1982) who applied NNMI in a limited area model.

Acknowledgments. The authors are grateful to Roger Daley, Ron Errico, Wayne Schubert and Joe Tribbia for their useful comments on an earlier version of the manuscript. The authors would also like to thank the anonymous reviewers for their comments, and in particular, for the suggestion to try the ECMWF initialization scheme. The manuscript was typed by Ursula Rosner.

REFERENCES

Adler, R. F., and E. B. Rodgers, 1977: Satellite-observed latent heat release in a tropical cyclone. *Mon. Wea. Rev.*, **105,** 956–963.

Andersen, J., 1977: A routine for normal mode initialization with nonlinear correction for a multi-level spectral model with triangular truncation. ECMWF Internal Rep. No. 15, 41 pp.

Baer, F., and J. Tribbia, 1977: On complete filtering of gravity modes through nonlinear initialization. *Mon. Wea. Rev.*, **105,** 1536–1539.

Ballish, B., 1981: A simple test of the initialization of gravity modes. *Mon. Wea. Rev.*, **109,** 1318–1321.

Briere, S., 1982: Nonlinear normal mode initialization of a limited area model. *Mon. Wea. Rev.*, **110,** 1166–1186.

Bourke, W., and J. L. McGregor, 1983: A nonlinear vertical mode initialization scheme for a limited area prediction model. *Mon. Wea. Rev.*, **111,** 2285–2297.

Daley, R., 1979: The application of nonlinear normal mode initialization to an operational forecast model. *Atmos.-Ocean,* **2,** 97–124.

DeMaria, M., and W. H. Schubert, 1984: Experiments with a spectral tropical cyclone model. *J. Atmos. Sci.*, **41,** 901–924.

Eliasen, E., B. Machenhauer and E. Rasmussen, 1970: On a numerical integration of hydrodynamical equations with a spectral representation of the horizontal fields. Dept. of Meteorology, Copenhagen University, 35 pp.

Elsberry, R., 1979: Applications of tropical cyclone models. *Bull. Amer. Meteor. Soc.*, **60,** 750–762.

Errico, R. M., 1983: Convergence properties of Machenhauer's initialization scheme. *Mon. Wea. Rev.*, **111,** 2214–2223.

Hoke, J. E., and R. A. Anthes, 1977: Dynamic initialization of a three-dimensional primitive equation model of Hurricane Alma of 1962. *Mon. Wea. Rev.*, **105,** 1266–1280.

Hovermale, J. R., and R. E. Livezey, 1977: Three-year performance characteristics of the NMC hurricane model. *Preprints, 11th Tech. Conf. Hurricanes and Tropical Meteorology,* Miami, Amer. Meteor. Soc., 122–124.

Kitade, T., 1983: Nonlinear normal mode initialization with physics. *Mon. Wea. Rev.*, **111,** 2194–2213.

Leith, C. E., 1980: Nonlinear normal mode initialization and quasi-geostrophic theory. *J. Atmos. Sci.*, **37,** 958–968.

Machenhauer, B., 1977: On the dynamics of gravity oscillations in a shallow-water model, with application to normal mode initialization. *Beitr. Phys. Atmos.*, **50,** 253–271.

——, 1979: The spectral method. *Numerical Methods Used in Atmospheric Models, Vol. II,* Chap. 3: GARP Publ. Ser. No. 17, 121–275.

Ooyama, K. V., 1969a: Numerical simulation of the life cycle of tropical cyclones. *J. Atmos. Sci.*, **26,** 3–40.

——, 1969b: Numerical simulation of tropical cyclones with an axisymmetric model. *Proc. WMO/IUGG Symp. on Numerical Weather Prediction,* Tokyo, III, 81–88.

Orszag, S. A., 1970: Transform method for the calculation of vector coupled sums: Application to the spectral form of the vorticity equation. *J. Atmos. Sci.*, **27,** 890–895.

Puri, K., and W. Bourke, 1982: A scheme to retain the Hadley circulation during nonlinear normal mode initialization. *Mon. Wea. Rev.*, **110,** 327–335.

Schubert, W. H., and M. DeMaria, 1985: Axisymmetric, primitive equation, spectral tropical cyclone model. Part I: Formulation. *J. Atmos. Sci.*, **42,** 1213–1224.

——, and J. J. Hack, 1982: Inertial stability and tropical cyclone development. *J. Atmos. Sci.*, **39,** 1687–1697.

Shea, D. J., and W. M. Gray, 1973: The hurricanes inner core region. I. Symmetric and asymmetric structure. *J. Atmos. Sci.*, **30,** 1544–1564.

Temperton, C., and D. L. Williamson, 1981: Normal mode initialization for a multilevel grid point model. Part I: Linear aspects. *Mon. Wea. Rev.*, **109,** 729–743.

Tribbia, J., 1981: Nonlinear normal mode balancing and the ellipticity condition. *Mon. Wea. Rev.*, **109,** 1751–1761.

Wergen, W., 1983: Initialization. *Interpretation of Numerical Weather Prediction Products, ECMWF Seminar/Workshop 1982,* 31–57. [Available from the European Centre for Medium Range Weather Forecasts, Shinfield Park, Reading RG2-9AX, England.]

Williamson, D. L., and C. Temperton, 1981: Normal mode initialization for a multilevel grid point model. Part II: Nonlinear aspects. *Mon. Wea. Rev.*, **109,** 744–757.